DRIFTING ELECTRON HOLES OBSERVED BY CRRES SPACECRAFT

M. A. Shukhtina, V. A. Sergeev, L. I. Vagina
Institute of Physics, University of St.Petersburg, Russia
e-mail: shuckht@snoopy.niif.spb.su

R. Rasinkangas, T. Bosinger, K. Mursula
Department of Physics, University of Oulu, Oulu, Finland

G. Kremser, A. Korth
Max-Planck-Institute fur Aeronomie, Katlenburg-Lindau, Germany

G. D. Reeves
Los Alamos National Laboratory, Los Alamos, USA

H. J. Singer
Space Environment Laboratory, NOAA, Boulder, USA

ABSTRACT

Short lived energy-dispersed decreases of the energetic electron flux (Drifting Electron Holes, DEHs) were previously found at geostationary orbit in association with sudden onsets of intense substorms. We surveyed well-defined DEH events in the dawn LT sector observed by the CRRES spacecraft which had an eccentric equatorial orbit with 6.3 Re apogee. Eleven out of 13 events were encountered at L>6.6 Re and 10 out of 13 events were observed under quiet or weakly disturbed (AE<300nT) conditions. Comparison with particle measurements at post-midnight geostationary LANL spacecraft was possible for 6 events observed by CRRES. Only in one case, when LANL and CRRES were at the same drift shell, DEH signatures were observed at both spacecraft. In all other cases (when the CRRES L-shell was located tailward of the geostationary orbit) we observed either no associated energetic particle response at 6.6 Re, or simultaneous particle injection. The results of this limited DEH survey show that the region of DEH formation is radially localized and DEHs preferentially occur at the periphery of the radiation belt (8-10 Re). When tracing back the energy dispersed DEHs according to the electrons' magnetic drift, we found the source location always near the midnight, and, if substorm onset could be identified, in the local time sector occupied by the Substorm Current Wedge. The abovementioned facts strongly support the interpretation of DEHs as being due to the inward plasma injection from the outer boundary of the radiation belt. We suggest that the decrease of the flux is basically due to the strong flux gradient near this outer boundary.

1. INTRODUCTION

Drifting Electron Holes (DEHs) are short-lived eastward drifting decreases of energetic electron fluxes in the outer radiation belt. Initially the DEHs were discovered at the geostationary LANL spacecraft [Ref. 1] at electron energies above ~300 keV. In contrast to the dropouts observed during the substorm growth phase near midnight (e.g. [Ref. 2]) , DEHs were found on the morningside after the onsets of intense substorms. It was suggested in [Ref. 1] that DEHs have the same origin as the ordinary particle injections, and that their peculiar characteristics reflect the spatial distribution of particle flux in the radiation belt.

The purpose of the this paper is a further study of such important characteristics of Drifting Electron Holes as

1. Longitudinal location of the DEH source
2. Radial dependence of DEH appearance and spatial relationship with particle injections
3. Temporal/spatial association with substorm onset and Substorm Current Wedge (SCW) position
4. Pitch-angle drift dispersion in the DEH events

2. OBSERVATIONS

We used for this study the measurements provided by Combined Release and Radiation (CRRES) spacecraft complemented by the data from geostationary LANL spacecraft. CRRES had a geostationary transfer eccentric orbit with 6.3 R_e apogee. The orbit inclination was 18.2^0 , so L-shells tailward of the geostationary orbit could also be crossed. We used data from Electron Proton Wide-Angle Spectrometer (EPAS) [Ref. 3]. EPAS measured electrons with energies 21.5-285 keV.

As compared to the energetic particle detectors at LANL spacecraft, EPAS detected fluxes at different pitch-angles with ~10° resolution.

13 morningside DEH events in August-December 1990 were identified using the EPAS quick-look plots. For six out of these 13 events data from geostationary LANL spacecraft were available. The list of the events is presented in Table 1. An example of a CRRES DEH event as well as simultaneous LANL electron data and AE index are shown in Figure 1.

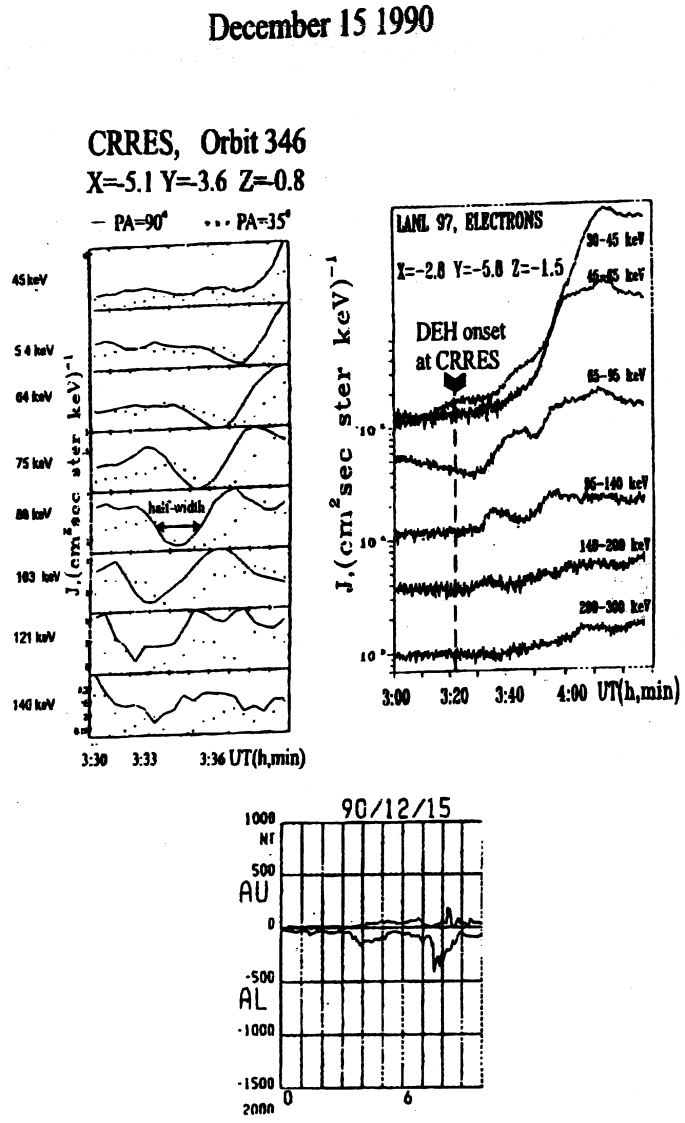

Figure 1. An example of CRRES DEH event (left), simultaneous electron injections at LANL (right) and corresponding AE index

2.1. Timing and location of DEH source.

As it was already mentioned, one of our goals was the evaluation of DEH onset times and estimation of the spatial location of the DEH source. The following technique was applied for this purpose.

At first step we determine the starting time of the DEH based on the observed energy dispersion. We assume that particles with the same pitch angle but different energies drift along the same path from the source to the spacecraft, so the time to reach the spacecraft is inversely proportional to their effective energy (relativistic effects are taken into account). Time UT_0 corresponding to infinite energy value is taken as the time of DEH origin (Fig.2a). According to the Table 1, the UT_0 value approximately (with accuracy of a few minutes) coincides with the substorm onset time, if the substorm could be identified.

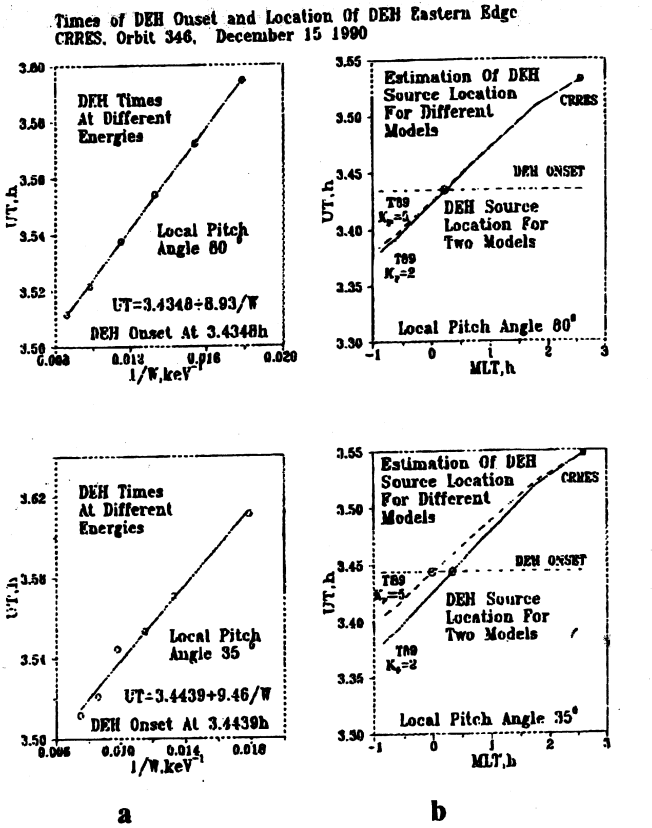

Figure 2. A scheme illustrating determination of DEH onset time (a) and DEH source location (b) for local pitch-angle values 80^0 (upper panels) and 30^0 (bottom panels) using different K_p versions of T89 models.

The second step is to compute the electron drift trajectory backward in time to find the particle position at time UT_0 which gives us the source location (Fig. 2b). Note that this procedure gives us only one point: *the source eastern edge* (if the DEH onset is considered) or *its center* (if we analyse the times of DEH minima). For illustration, we estimate the width of the DEH region as the distance which particle passes during the time equal to the DEH half-width (Fig. 1). The results of calculations are presented in the Table 2. The same technique was applied to find the onset times and the source location of particle injections seen in LANL data (see below).

Table 1 Summary of information for the DEH events observed at CRRES (and LANL) spacecraft.

Date	Ground activity	AE,nt	Ground onset, UT	CRRES MLT, hours	K_p	R,R_e	DEH onset, UT	LANL MLT, hours	K_p	R,R_e	DEH or INJ	DEH/INJ onset,UT
Aug 17	substorm	500	13:17	5.8	1 5	6.4 6.7	13:19	2.0	1 5	6.6 6.8	DEH	13:17
Sept 19	weak background	100	no onsets	5.4	1 5	8.1 10.4	10:54	no data				
Sept 26	disturb. mostly in AU; SC	150	SC at 9:54	4.6	2 5	7.9 10.2	9:53	10.4 22.9	1 5 1 5	6.6 6.6 6.6 6.6	—	—
Sept 26	weak substorm	150	~10:20	5.0	1 5	8.3 11.0	10:15	11.0 23.5	1 5 1 5	6.6 6.6 6.6 6.6	—	—
Sept 29	weak substorm	150	8:47-8:50	5.7	2 5	8.6 9.9	8:51	no data				
Oct 4	substorm	500	5:36	5.2	1 4	7.6 8.2	5:34	no data				
Oct 6	substorm	500	~5:50	3.9	2 5	6.5 7.8	5:46	no data				
Oct 14	growth phase	~100	~13:06	6.3	3	8.7	13:04	no data				
Nov 8	quiet	~0	no onsets	4.2	2 4	7.9 8.5	4:13	4.7 19.2	1 5 1 5	6.6 6.6 6.6 6.6	— —	— —
Nov 8	growth phase	~100	~4:50	4.6	2 4	7.9 8.4	4:51	5.4 19.9	1 5 1 5	6.6 6.6 6.6 6.6	— INJ	—
Nov 12	weak substorm	<50	~7:00	4.4	2 4	9.4 10.2	7:00	no data				
Nov 17	growth phase	~200	no onsets	4.2	1 5	7.7 8.5	6:33	no data				
Dec 15	substorm	150	3:26	2.6	2 5	7.4 7.9	3:26	4.0 18.5	1 5 1 5	6.6 6.6 6.6 6.6	INJ —	3:26 —

One limitation of this method concerns the magnetic field model used. We choose the version of model by comparing actual magnetic field measurements at CRRES spacecraft with magnetic field computed from the Tsyganenko-89 model [Ref. 4]. To make sure we also made drift calculations for quiet and disturbed K_p values

Table 2

Date	CRRES K_p	DEH_{min} coord. MLT, hours R,R_e		DEH_{min} onset, UT
Aug 17	1 5	2.8 1.9	6.3 6.9	13:21
Sept 19	1 5	3.9 3.5	8.2 10.8	10:58
Sept 26	2 5	2.2 1.8	8.0 10.5	9:53
Sept 26	1 5	4.3 4.2	8.3 11.2	10:15
Sept 29	2 5	1.4 1.2	8.8 10.7	8:52
Oct 4	1 4	5.0 5.0	7.6 8.2	5:33
Oct 6	2 5	3.9	6.5 7.8	5:47
Oct 14	3	6.3	8.7	13:08
Nov 8	2 4	4.2	7.9 8.5	4:12
Nov 8	2 4	4.6	7.9 8.4	4:54
Nov 12	2 4	4.4	9.4 10.2	7:04
Nov 17	1 5	4.2	7.7 8.5	6:36
Dec 15	2 5	2.6	7.4 7.9	3:29

(see Table 2). In most of the runs we computed drifts for particles with local pitch angle 80°, but a special study of pitch-angle dispersion was also done.

2.2. Comparison of CRRES and LANL data

For six of considered 13 events we also had data from geostationary LANL spacecraft. Contrary to our expectations, we found well defined simultaneous DEH feature at LANL spacecraft only in one event (August 17, Fig.3a). In two cases (November 8 and December 15) data from LANL spacecraft showed the injection signatures (see an example in Figure 1). In remaining 3 cases no effects were detected at geostationarty orbit. This information is also presented in Table 1.

Comparison of spacecraft radial positions gives some explanation to these results. In the only case when the DEH was observed by both spacecraft they were on the same L-shell, and analysis of both data sets showed the same longitudinal position of the DEH source. In all other events the CRRES's L-shell was situated earthward of the LANL shell (Table 1). Therefore, results reveal the severe radial localization of the drift shell where the DEHs can be observed.

Spatial configurations for two representative events are illustrated in details in Figure 3. It shows the spacecraft positions (mapped to the equatorial plane) when they detect the DEH/injection events as well as the DEH/ injection source locations in this plane computed for different K_p values. On these plots we also show the local times of Substorm Current Wedge (SCW) boundaries determined from midlatitude magnetic variations (as described in [Ref.5]).

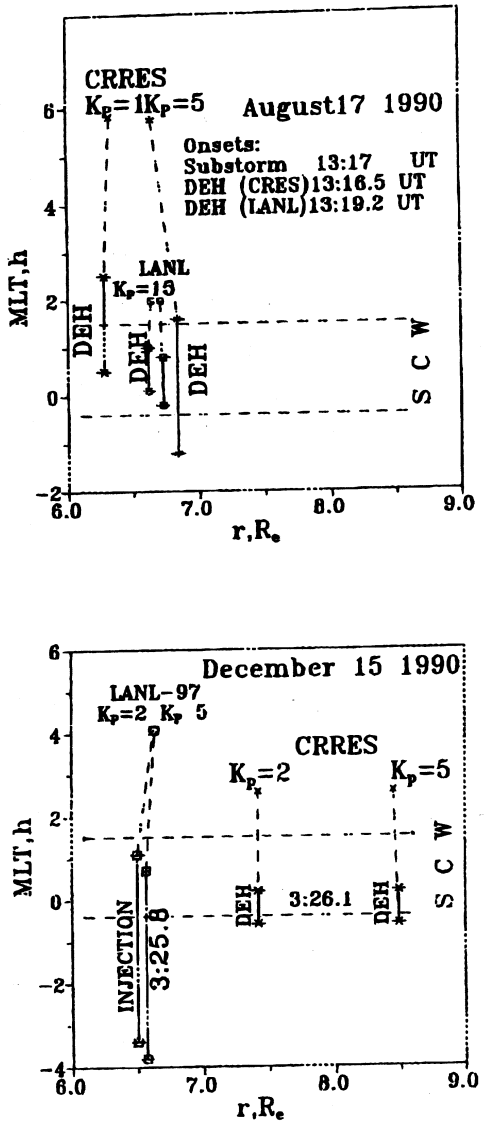

Fig. 3. Onset times and positions of DEHs and injections observed by CRRES and LANL spacecraft for two K_p models for substorm events on August 17 (upper panel) and December 15 (lower panel).

Following conclusions can be made from Figure 3.

(1) The times of DEH onsets and injection onsets nearly coincide with the substorm onset time (1317 UT on August 17 and 0326 UT on December 15).
(2) When the DEH is observed by both spacecraft (August 17), the radial and longitudinal positions of the DEH source, determined for each spacecraft separately, agree with each other. In local time they nearly coincide with the SCW location.
(3) When the injection was observed by LANL while CRRES detected the DEH (December 15, see Fig.1), the longitudinal positions of the injection source and DEH source approximately corresponded to each other (with more narrow DEH source region in the morningside part of injection region), and both are in agreement with the SCW position. Radial positions are, of course, different: the injection originates ~1-2 R_e earthward of the DEH.

Close association of the source position (in MLT) and onset times of the Drifting Electron Holes with substorms is very distinct in these events. However, according to Table 1, quite often we did not find any considerable activity in association with the DEHs. We assume that in these cases the physics is the same, but the substorm-like activations were so weak (pseudobreakups,[Ref. 6]) that they could not be detected on the ground.

2.3. Summary of survey of DEH events

We summarize the results presented in the Tables 1,2 as follows.

- When substorm onsets could be identified, the DEH starting time coincided with substorm onset within the accuracy of timing the onset (Aug. 17, Dec. 15, Sept.26, Oct.6, Sept.29, Nov.12, Oct.4).
- In all considered events the Drifting Electron Holes start close to midnight (see Table 2).
- When the SCW position could be determined (August 17, December 15), the DEH source appears in the local time sector occupied by the Substorm Current Wedge. In the remaining cases the DEH source always occurs in the near midnight-early morning sector, i. e. in the region where the substorm activations are most frequent.
- DEHs in our survey often have very weak geomagnetic activity associated.
- Most frequently the DEH source appears at geocentric distances outside the geostationary orbit (r~ 8-10 R_e).

These results can be understood assuming that :
(a) both the DEH events and injection events are generated by substorm activations ;
(b) the DEHs originate in a radially confined region close to the outer boundary of the radiation belt, while the same process forms the flux increase (injection signature) on the inner drift shell;
(c) transient weak substorm activations (pseudobreakups) are sufficient to generate the Drifting Electron Holes.

2.4 Pitch-angle dispersion in the DEHs

Figure 1 shows a clear example of pitch-angle dispersion in the Drifting Electron Hole (this effect was not shown in the previous papers). Computation of drift trajectories for different pitch-angles (Figure 2, for local pitch angles 35° and 80°) shows very close onset times and source local times for both groups of particles, confirming quantitatively the drift origin of pitch-angle dispersion.

3. SUGGESTED MECHANISM TO FORM THE DRIFTING ELECTRON HOLES

Strong preference of DEH occurrence to the outer boundary of the radiation belt (8-10 R_e) supports the gradient mechanism of DEHs formation suggested in [Ref. 1]. When modelling the particle flux variation caused by a burst of earthward convection at substorm onset, a radial gradient of electron flux [Ref. 7] (modelled here as $j \sim \exp[-kr]$) should be taken into account. Assuming an exponential energy spectrum, the background particle distribution is described as

$$j = c \times \exp[-E/E_0 - kr]$$

According to Liouville's theorem

$$j / E \cong \text{const}$$

Consider a particle injected from the initial point r_1 to the final position r_2 ., which is accelerated from initial energy E_1 to the final energy E_2 (we observe particles at energy E2 at the final point, at spacecraft position). It gives us the observed (injected) particle flux as

$$j_f(r_2,E_2) = E_2/E_1 \times j_i(r_1,E_1) = \\ = E_2/E_1 \times c \times \exp[-E_1/E_0 - kr_1]$$

This injected particle flux should be compared with the flux at the same energy and same point observed prior to the injection

$$j_f(r_2,E_2) / j_i(r_2,E_2) = E_2/E_1 \times \exp[(E_2-E_1)/E_0 - k(r_1-r_2)]$$

One can see that two terms ($[E_2-E_1]/E_0$ and $k[r_1-r_2]$) have the opposite signs, so the flux variation resulting from particle injection can be positive (injection) or

negative (DEH). The preferential condition to have the DEH-like response is a flat energy spectrum (large E_o) and large flux gradient. According to our estimates (not shown here), both conditions are probably satisfied for energetic electrons at the outer boundary of the radiation belt.

4. CONCLUSIONS

- We demonstrate examples of pitch-angle drift-related dispersion in the DEH (in addition to previously reported drift energy dispersion) and show that DEHs sometimes can be found at energies as low as ~50 keV.
- We confirm that DEH generation often coincides with substorm onsets (in both space and time), but show that very weak activations are also efficient to generate the DEHs.
- DEHs have a strong preference to appear near the outward L-shell limit sampled by CRRES spacecraft (L~8-10 Re), i.e. near the outer boundary of the radiation belt electrons.
- Simultaneous observations by CRRES and LANL spacecraft revealed: (1) the severe radial localization of DEH signatures and (2) appearance of ordinary injection signatures at the more earthward drift shell.
- Detailed study of one event (Dec. 15) showed that azimuthal locations of simultaneously observed DEHs and injections nearly coincide, and both agree with the position of the Substorm Current Wedge activated at substorm onset.

These characteristics essentially confirm the model [Ref. 1] (see Section 3) in which both DEH and injection signatures in the energetic particle flux are formed by the Earthward plasma injection in the presence of the sharp flux gradient existing at the outer boundary of the radiation belt.

5. ACKNOWLEDGEMENT

The work of three of us (M.A.S, V.A.S, L.I.V.) was supported by Russian Foundation of Basic Research grant N 96-05-64019. M.A.S thanks the University of Oulu for their financial support during her stay in Oulu.

6. REFERENCES

1. Sergeev V A & al 1992, Drifting Electron Holes in the energetic electron flux at geosynchronous orbit following substorm onset, *J. Geophys. Res.*, 97, 6541-6548

2. Baker D N & al 1982, Observations and modelling of energetic particles at synchronous orbit on July 29, 1977, *J. Geophys. Res., 87, 5917-5932*

3. Korth A & al 1992, The electron and proton wide-angle spectrometer (EPAS) on the CRRES spacecraft, *J. of Spacecraft and Rockets*, 29,609-614

4. Tsyganenko N A 1989, A magnetospheric magnetic field with a warped tail current sheet, *Planet. Space Sci.*, 37, 5-20

5. Vagina L I & al 1996, Use of mid-latitude magnetic data for modelling and diagnostics of magnetospheric substorms, *Adv. Space Res.*, 18, 229-232

6. Koskinen H E J & al 1993, Pseudobreakup and substorm growth phase in the ionosphere and magnetosphere, *J. Geophys. Res.*, 5801-5813

7. Imhof W L & al 1993, The outer boundary of the Earth's Electron Radiation Belt: dependence upon L, energy and equatorial pitch angle, *J. Geophys. Res.*, 5925-5934